OXFORD

Human Molecular Genetics, 2017, Vol. 26, No. 22 4416–4428

doi: 10.1093/hmg/ddx327
Advance Access Publication Date: 21 August 2017
Original Article

ORIGINAL ARTICLE

FOXOs modulate proteasome activity in human-induced pluripotent stem cells of Huntington's disease and their derived neural cells

Yanying Liu[1], Fangfang Qiao[1], Patricia C. Leiferman[2], Alan Ross[2], Evelyn H. Schlenker[1] and Hongmin Wang[1,*]

[1]Division of Basic Biomedical Sciences, Sanford School of Medicine, University of South Dakota, Vermillion, SD 57069, USA and [2]Sanford Medical Genetics Laboratory, Sioux Falls, SD 57105, USA

*To whom correspondence should be addressed at: Division of Basic Biomedical Sciences, Sanford School of Medicine, University of South Dakota, Vermillion, SD 57069, USA. Tel: 1 6056586382; Fax: 1 6056776381; Email: hongmin.wang@usd.edu

Abstract

Although it has been speculated that proteasome dysfunction may contribute to the pathogenesis of Huntington's disease (HD), a devastating neurodegenerative disorder, how proteasome activity is regulated in HD affected stem cells and somatic cells remains largely unclear. To better understand the pathogenesis of HD, we analyzed proteasome activity and the expression of FOXO transcription factors in three wild-type (WT) and three HD induced-pluripotent stem cell (iPSC) lines. HD iPSCs exhibited elevated proteasome activity and higher levels of FOXO1 and FOXO4 proteins. Knockdown of FOXO4 but not FOXO1 expression decreased proteasome activity. Following neural differentiation, the HD-iPSC-derived neural progenitor cells (NPCs) demonstrated lower levels of proteasome activity and FOXO expressions than their WT counterparts. More importantly, overexpression of FOXO4 but not FOXO1 in HD NPCs dramatically enhanced proteasome activity. When HD NPCs were further differentiated into DARPP32-positive neurons, these HD neurons were more susceptible to death than WT neurons and formed Htt aggregates under the condition of oxidative stress. Similar to HD NPCs, HD-iPSC-derived neurons showed reduced proteasome activity and diminished FOXO4 expression compared to WT-iPSC-derived neurons. Furthermore, HD iPSCs had lower AKT activities than WT iPSCs, whereas the neurons derived from HD iPSC had higher AKT activities than their WT counterparts. Inhibiting AKT activity increased both FOXO4 level and proteasome activity, indicating a potential role of AKT in regulating FOXO levels. These data suggest that FOXOs modulate proteasome activity, and thus represents a potentially valuable therapeutic target for HD.

Introduction

Huntington's disease (HD) is an incurable inherited neurodegenerative disorder resulting from an abnormal expansion of CAG trinucleotide repeats in exon 1 of the huntingtin (Htt) gene (1). Typically, normal people have 35 or fewer CAG repeats in exon 1 of the Htt gene, while patients with HD have 36–120 or more CAG repeats in the gene (2). The severity and age at onset of the disorder are correlated with CAG repeat length: longer CAG repeat size is associated with earlier onset of age and more severe symptoms (3). Neuropathologically, HD is characterized by progressive neurodegeneration primarily in the striatum and to less degree, in the cortex, and by formation of Htt protein aggregates (inclusions) that contain misfolded Htt and Htt interacting molecules in neurons (4). In HD affected striatum, the γ-aminobutyric acid (GABA)ergic medium-sized spiny neurons (MSNs) positive in DARPP32 staining are the most vulnerable

Received: July 25, 2017. **Revised:** August 13, 2017. **Accepted:** August 17, 2017

neuronal subtype population to mutant Htt (5). It is uncertain why mutant Htt cannot be efficiently degraded and why it is toxic to neurons, especially MSNs in the striatum.

The ubiquitin-proteasome system (UPS) plays a vital role in cell survival and death, cell proliferation, and signal transduction, while the UPS itself is highly regulated by numerous factors (6–8). Importantly, many previous studies investigating whether UPS function is impaired in HD have not offered a conclusive answer. On one hand, several studies reported that UPS dysfunction occurs in many brain regions and in skin fibroblasts derived from patients with HD (9), in the isolated synaptosomes in the R6/2 HD mice (10), and in the cell models of HD (11). In contrast, other investigations have found no inhibition of 20 S proteasome activity in the Tet/HD94 inducible mouse model (12) and in R6/2 mice (13). Intriguingly, studies from the full-length Htt YAC72 HD mouse model showed impaired-proteasome activity during the post-symptomatic stage, similar to the results obtained from the brains of patients with HD (14). Over the last decade, human HD induced pluripotent stem cells (iPSCs) have been become increasingly favored models for understanding the pathogenesis of the disease. However, proteasome functionality in the HD iPSCs and their derived neural cells has not been investigated.

FOXO proteins are a subgroup of the Forkhead transcription factors characterized by a conserved DNA-binding domain known as the 'Forkhead box', or FOX (15). Mammalian cells including human cells encode four FOXO proteins, FOXO1, FOXO3a, FOXO4 and FOXO6. These transcription factors act downstream of insulin signaling and play important roles in longevity, metabolism, cellular proliferation and stress tolerance (16). Increasing data also suggest that FOXOs modulate UPS by altering the expression of some tissue specific ubiquitin E3 ligases (15) or proteasome subunit expression (17). Despite these studies, the role of FOXOs in the condition of HD and in HD iPSCs remains less explored. Here, we generated several human HD iPSC lines and examined the role of FOXOs in regulating proteasome activity in the HD iPSCs and their derived neural cells.

Results

The HD iPSCs showed higher levels of proteasome activity than the wild-type (WT) iPSCs

Using previously described methods that employed episomal vector-mediated iPSC reprogramming (18–20), we generated several iPS cell lines from human fibroblasts, which included three WT cell lines (referred to as 16Q, 18Q, and 19Q) and four HD iPS cell lines (referred to as 46Q, 69Q, 70Q, and 99Q) (Table 1). After being manually picked and expanded on Matrigel in a stem cell growth medium, these iPSCs showed typical human embryonic stem cell morphologies, including being tightly packed and having smooth distinct edges (Fig. 1A, left). After staining for a stem cell-specific marker, alkaline phosphatase, the iPSCs showed alkaline phosphatase-positive staining (Fig. 1A, right). In addition, following immunocytochemical staining of the iPSCs with stem cell-specific antibodies, the cells were also positive for other markers of pluripotency (Fig. 1B). G-banding chromosomal analysis confirmed that these cells had normal karyotypes (Fig. 1C). After injection into immunocompromised mice, the iPSCs formed teratomas containing cells and tissues of all three germ layers (Fig. 1D), suggesting that these iPSCs had pluripotent capability. PCR analysis of the iPSCs passaged over 20 times showed no evident transgene expression (data not shown), indicating that the cell lines had lost the episomal vectors.

Table 1. Analyzed CAG repeat and karyotype results in the generated iPSC lines

Genotypes	iPSC line	Patient phenotype	Sex	Karyotype	CAG #
WT	16Q	Healthy	M	46, XY	15/16
	18Q	Healthy	M	46, XY	10/18
	19Q	Healthy	M	46, XY	19/19
HD	46Q	HD	M	46, XY	20/46
	69Q	HD	F	46, XX	15/69
	70Q	HD	F	46, XX	17/70
	99Q	HD	M	46, XY	22/99

Appropriate proteasome activity plays an important role in maintaining pluripotency of stem cells (17). To better understand the role of the proteasome in reprogramming HD somatic cells into iPSCs, we measured the three types of peptidase activities of the proteasome, namely chymotrypsin-like, caspase-like, and trypsin-like proteolytic activities, in the three WT (16Q, 18Q, and 19Q) and three HD fibroblasts (46Q, 70Q and 99Q) that were used for reprogramming. Compared to the three types of WT fibroblasts, all of the three types of peptidase activity of the proteasome were reduced in the three types of HD fibroblasts (Fig. 1E). By contrast, following reprogramming the three HD iPS cell lines showed increased proteolytic activities compared to the WT cell lines (Fig. 1F). Interestingly, the total ubiquitinated (Ub) protein levels in the HD iPSCs did not significantly differ from those of the three WT iPSC lines (Fig. 1G and H). Increased proteasome activity in HD iPSCs was further supported by increased-turnover of the SOX2 protein, a previously verified proteasome substrate (21), in HD iPSCs compared to that in control iPSCs (Fig. 1I and J). Thus, HD iPSCs show higher levels of proteasome activity than WT iPSCs.

FOXO4 is required for elevated proteasome activity in HD iPSCs

Since previous data have shown that FOXO transcription factors may regulate proteasome activity in stem cells (17), we therefore analyzed FOXO protein expression levels in both HD and WT iPSCs. As shown in Figure 2A and B, FOXO1 and FOXO4 protein levels in the three HD iPSC line were significantly higher than those in the three WT iPSC lines. In contrast, FOXO3a and FOXO6 expressions in HD iPSCs did not significantly differ from those in WT iPSCs (Fig. 2A and B). To further examine whether both FOXO1 and FOXO4 were required for enhanced proteasome activity, we performed lentiviral small hairpin RNA (shRNA)-mediated FOXO knockdown experiments in HD iPSCs. Following knockdown of FOXO1 expression, we did not observe reduced proteasome activity in the cells (data not shown). However, knockdown of FOXO4 (Fig. 2C and D) remarkably reduced all of the three types of proteasome activities (Fig. 2E). Therefore, although elevated proteasome activity in HD iPSCs is associated with increased expression levels of both FOXO1 and FOXO4, only FOXO4 is required for elevated proteasome activity.

HD iPSCs-derived neural progenitor cells (NPCs) show reduced proteasome activity and decreased FOXO1 and FOXO4 expressions compared to WT NPCs

We next differentiated the three lines of HD iPSCs and the three lines of WT iPSCs into NPCs. Both HD and WT NPCs were highly proliferative and expressed neural progenitor markers,

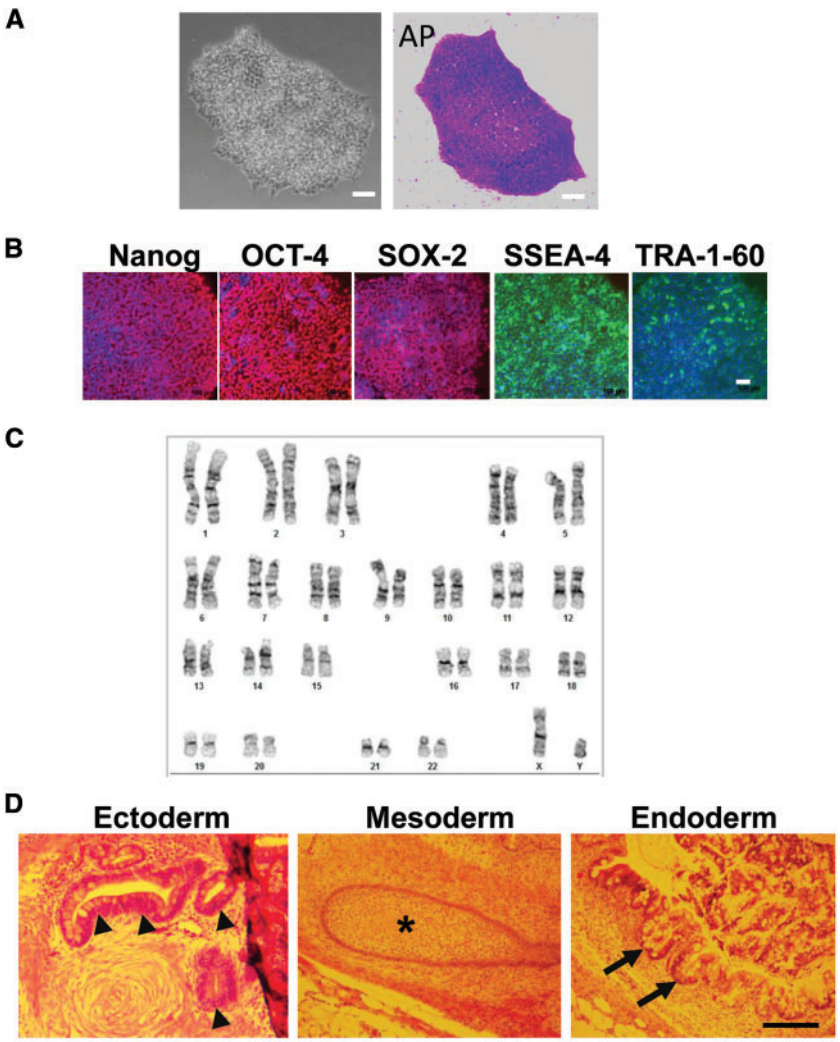

Figure 1. HD iPSCs show increased proteasome activity compared with WT iPSCs. (**A**) Representative image of a generated HD iPSC colony under a phase contrast microscope (left) and the alkaline phosphatase-stained colony positive for AP staining (right). Scale bar, 100 μm. (**B**) Immunocytochemistry of a representative HD iPSC line with the stem cell-specific markers as indicated. Hoechst 33342 was used to counter-stain nuclei (blue). Scale bar, 100 μm. (**C**) A representative G-banded karyogram of chromosomes from an HD iPSC line showing normal karyotype. (**D**) Representative H & E stained teratoma sections derived from an HD iPSC line following injection into immune-compromised mice depicting different tissue types. Arrow heads in the left panel (ectoderm) indicating neural tubes; asterisk in the middle panel (mesoderm) showing cartilage; arrows in the right panel (endoderm) indicating intestinal epithelia. Scale bar, 100 μm. (**E**) The three types of proteasome activity (in arbitrary unit, A.U.) measured from three WT controls (Con) and three HD human fibroblast cells. (**F**) The three types of proteasome activity measured from three lines of WT iPSCs (Con) and three lines of HD iPSCs (HD). (**G**) Western blot analysis of ubiquitinated (Ub) proteins in the iPSCs. Actin was used as a loading control. (**H**) Quantitative analysis of (G). All numerical data are shown as mean ± SD; $n = 3$–6. $^{*}P < 0.05$, $^{**}P < 0.01$, $^{***}P < 0.001$, $^{****}P < 0.0001$. (**I**) Cycloheximide (CHX) chase analysis of the degradation of a proteasome substrate, SOX2. Control or HD iPSCs were treated with 50 μg/ml CHX and the cell lysates were collected at the indicated time points (in hours) for Western blot analysis of SOX2. Top panel, SOX2 protein degradation in WT iPSCs; lower panel, SOX2 protein degradation in HD iPSCs at the indicated time points. (**J**) Quantification of the relative levels of SOX2 shown in (I). Data are shown as mean ± SD; $n = 3$. $^{***}P < 0.001$, $^{****}P < 0.0001$.

including Doublecortin (DCX), Nestin and SOX2 (Fig. 3A). Expression of mutant Htt did not affect neural induction, as both HD and WT iPSCs showed similar expression of the neural progenitor markers (data not shown). Following neural induction, however, HD NPCs displayed lower proteasome activity than WT NPCs (Fig. 3B). The reduced proteasome activity in the HD NPCs was also associated with the increase of Ub proteins (Fig. 3C and D), and with the reduced turnover of the proteasome substrate, SOX2 (Fig. 3E and F). Intriguingly, in contrast to HD iPSCs, in which both FOXO1 and FOXO4 expressions were upregulated (Fig. 2A and B), HD NPCs showed reduced FOXO1 and FOXO4 levels compared to WT NPCs (Fig. 3G and H). Thus, after iPSCs are differentiated into NPCs, HD NPCs show reduced proteasome activity and decreased FOXO1 and FOXO4 expressions compared with their WT counterparts.

Overexpression of exogenous FOXO4 but not FOXO1 increases proteasome activity in HD NPCs

As reduced proteasome activity in HD NPCs is associated with decreased FOXO4 expression, we next examined whether overexpression of the transcription factor would enhance proteasome activity in HD neural cells. We therefore transfected HD NPCs with a FOXO4 expression plasmid (Fig. 4A). Transient overexpression of FOXO4 led to increased proteasome activity in the HD NPCs (Fig. 4B), which was confirmed by the enhanced

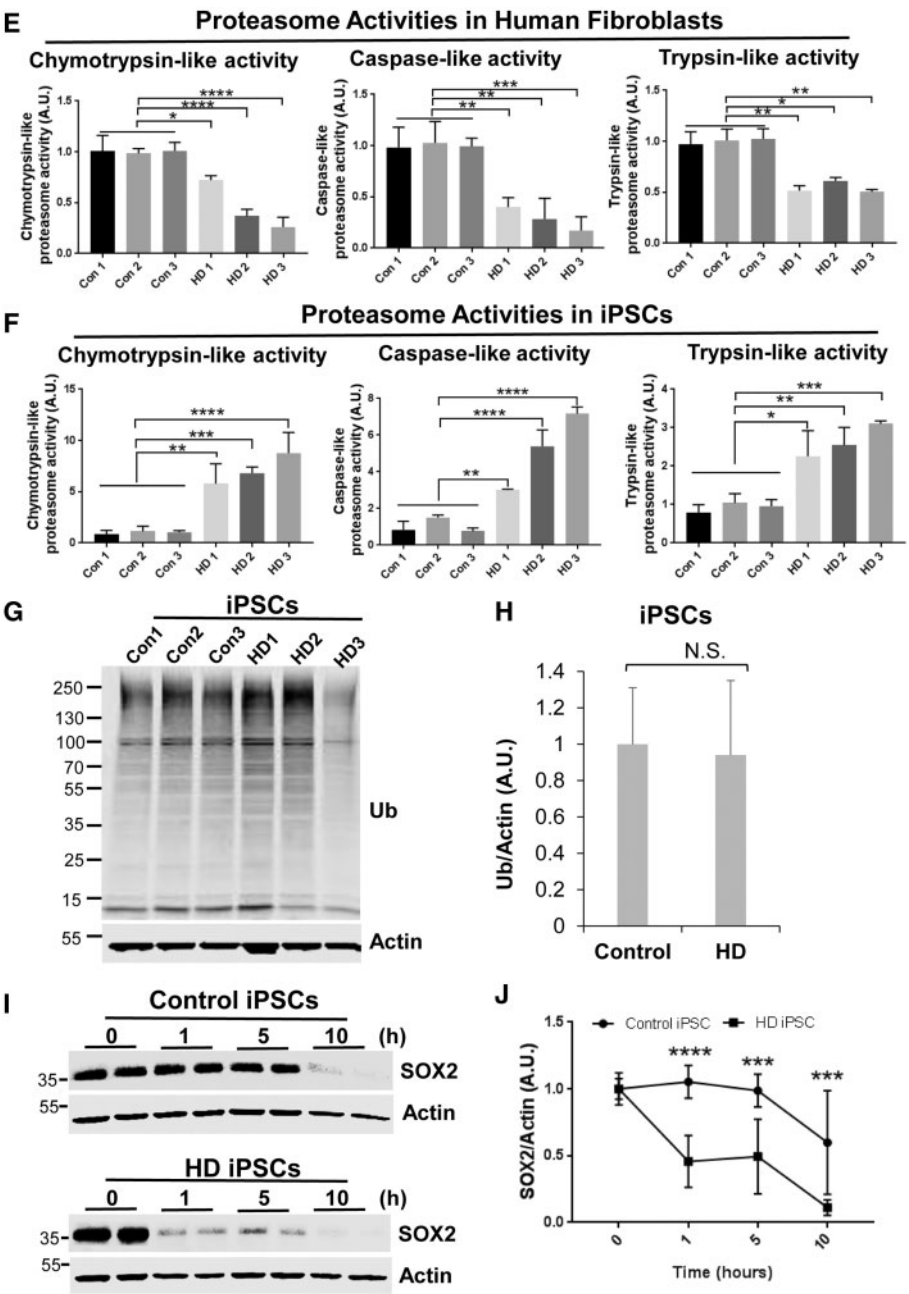

Figure 1. Continued

degradation of the proteasome substrate, SOX2, in the HD cells transfected with FOXO4 (Fig. 4C and D). Transfection of FOXO4 in HD NPCs also increased intracellular ATP level (Fig. 4E). These data indicate that FOXO4 positively regulates proteasome activity in HD NPCs.

HD iPSC-derived neurons show reduced proteasome activity and decreased FOXO4 expression compared to WT iPSCs-derived neurons

We then further differentiated the NPCs into neurons and stained the cells with various neuronal markers. After 60 days of neuronal differentiation, we were able to differentiate the NPCs into neurons positive in expressions of Tuj1, GABA and DARP32, a specific marker for MSNs (22) (Fig. 5A). Although HD neurons showed decreased viability without any treatment, exposure of the neurons to an oxidative stress inducer, menadione (MD) (23), dramatically enhanced cell death (data not shown). In normal culture condition, no evident Htt aggregate was observed under a fluorescence microscope (data not shown). Following MD-induced oxidative stress, some neurons positive for MAP2 staining exhibited small but evident aggregates (Fig. 5B), which were confirmed by the filter trap assay (Fig. 5C). Thus, HD iPSC-derived neurons replicate, especially under oxidative stress, the two major neuropathological features, neuronal death and formation of Htt aggregates.

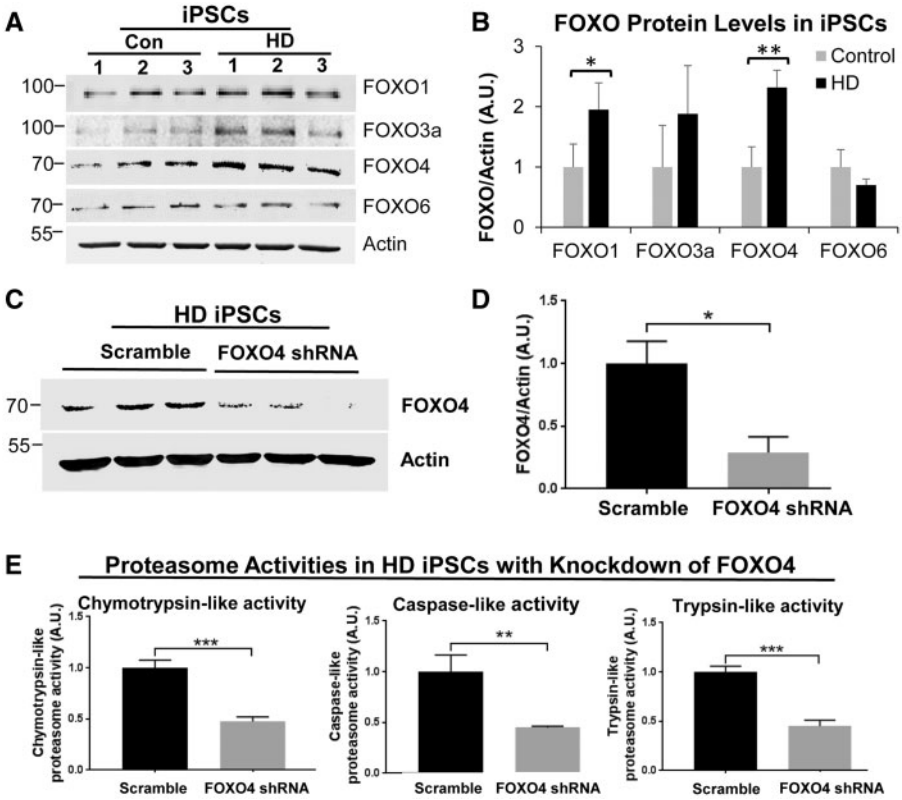

Figure 2. FOXO4, but not FOXO1, is required for elevated proteasome activity in HD iPSCs. (**A**) Western blot analysis of FOXO protein expressions in iPSCs. (**B**) Quantitation of (A). (**C**) Western blot analysis of FOXO4 protein level in HD (99Q) iPSCs to verify knockdown of the protein expression. (**D**) Quantitative analysis of FOXO4 expression from (C). (**E**) Three types of proteasome activity in the HD iPSCs treated either with lentiviral scramble or FOXO4 shRNAs. All numerical data are shown as mean ± SD; $n = 3$–6. $^{*}P < 0.05$, $^{**}P < 0.01$, $^{***}P < 0.001$.

We next examined whether HD iPSC-derived neurons was associated with altered proteasome activity observed in other HD models. To do so, we compared the three types of proteasome activity in two lines of HD iPSC-derived neurons (46Q and 99Q) with two lines of WT iPSC-derived neurons (16Q and 18Q). Our results showed that proteasome activities in the HD iPSC-derived neurons were dramatically lower than those in WT iPSC-derived neurons (Fig. 5D). The reduced proteasome activities in HD neurons were also reflected by increased accumulation of Ub proteins (Fig. 5E and F), and by delayed degradation of a proteasome substrate, SOX2, in the cells (Fig. 5G and H). To determine whether reduced proteasome activity was associated with altered FOXO1 and FOXO4 expressions, we examined the two protein levels in both HD and WT iPSC-derived neurons. Similar to HD NPCs, HD neurons expressed a relatively lower level of FOXO4 than the WT neurons, while FOXO1 protein level in the HD neurons did not significantly differ from that in WT neurons (Fig. 5I and J). Thus, HD iPSC-derived neurons show reduced proteasome activity and a decreased FOXO4 protein level compared to WT iPSC-derived neurons.

AKT regulates FOXO4 in HD cells

As activation of the serine/threonine kinase, AKT, promotes degradation of FOXOs (24), we asked whether AKT signaling might be altered in HD iPSCs and their derived neurons. We therefore examined the levels of the total AKT and activated AKT (phosphylated at Thr-308) in the three HD iPS cell lines by immunoblotting (Fig. 6A). Levels of total AKT did not change significantly in HD iPSCs compared with WT controls (Fig. 6A and B). On the contrast, protein levels of phosphorylated AKT (p-AKT) were dramatically reduced in HD iPSCs (Fig. 6A and B). Interestingly, levels of both total AKT and activated AKT did not change in HD NPCs compared with WT NPCs (data not shown). Although levels of total AKT did not change in the HD iPSC-derived neurons compared with those in WT neurons (Fig. 6C and D), p-AKT levels were significantly increased in the HD iPSC-derived neurons (Fig. 6D).

To further determine whether AKT is causative in regulating FOXO4, we treated HD neurons with a selective AKT inhibitor, MK-2206 (25), and then examined FOXO4 protein level. As shown in Figure 6E and F, inhibition of AKT by MK-2206 significantly increased FOXO4 protein level in the treated HD neurons. Moreover, this was associated with elevated proteasome activities following MK-2206 treatment (Fig. 6G). Since AKT signaling negatively regulates FOXO4, these results indicate that reduced AKT activation is likely responsible for increased FOXO4 protein levels in HD iPSCs, while elevated AKT activation is attributed to decreased FOXO4 protein level in HD neurons.

Discussion

The role of UPS in the pathogenesis of HD remains contentious. Here we demonstrate that the HD iPSCs and their derived neural cells exhibit differential proteasome activities compared to their WT counterparts. Before neural differentiation, HD iPSCs exhibited elevated proteasome activity, and increased expressions of FOXO1 and FOXO4 compared to the WT iPSCs. Knockdown of

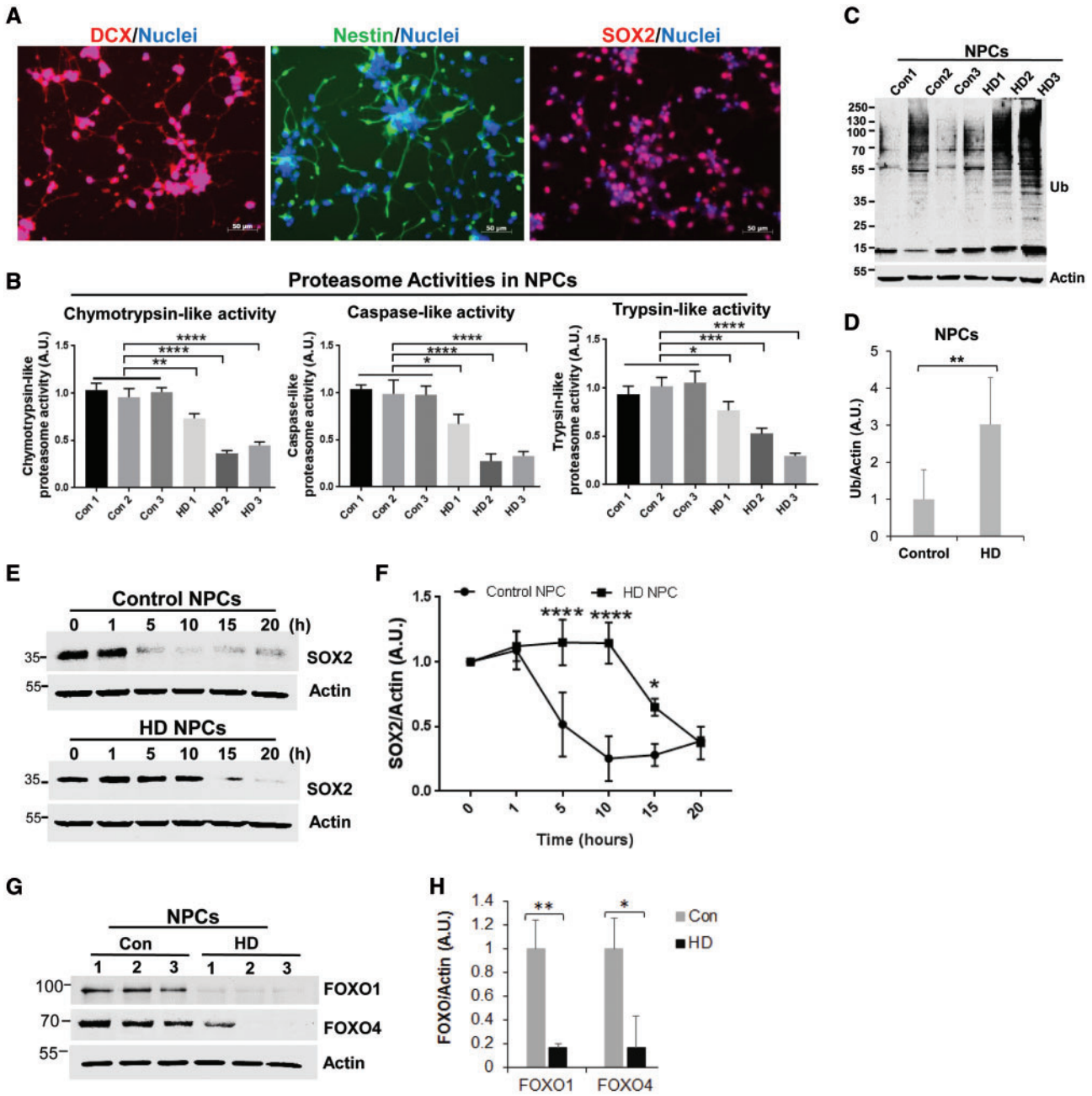

Figure 3. HD iPSC-derived NPCs show decreased proteasome activity and reduced levels of FOXO1 and FOXO4 proteins compared with WT iPSC-derived NPCs. (**A**) Immunostaining of NPC cells with the NPC markers as indicated. Scale bar: 50μm. (**B**) Measurement of three types of proteasome activity in three lines of WT (Con) and three lines of HD NPCs. (**C**) Western blot analysis of Ub-protein levels in NPCs. (**D**) Quantitative results measured from experiment (C). (**E**) CHX chase analysis of the degradation of SOX2. Control or HD NPCs were treated with 200 μg/ml CHX and the cell lysates were collected for Western blot analysis of SOX2 at the indicated time points. Top panel, SOX2 protein degradation in WT NPCs; lower panel, SOX2 protein degradation in HD NPCs at the indicated time points. (**F**) Quantification of the relative levels of SOX2 shown in (E). Data are shown as mean ± SD; $n = 3$. $^{*}P < 0.05$, $^{****}P < 0.0001$. (**G**) Western blot analysis FOXO1 and FOXO4 protein levels in NPCs. (**H**) Quantitative analysis of (G). All numerical data are shown as mean ± S.D; $n = 3$–6. $^{*}P < 0.05$, $^{**}P < 0.01$, $^{***}P < 0.001$, $^{****}P < 0.0001$.

FOXO4 but not FOXO1 decreased proteasome activity in HD iPSCs. Following neural differentiation, the HD iPSC-derived NPCs and neurons exhibited lower levels of proteasome activity and FOXO4 expression than their WT counterparts. More importantly, overexpression of FOXO4 in HD NPCs dramatically enhanced proteasome activity and promoted HD NPC survival. We also determined a negative association relationship between AKT activation and FOXO4 levels in both HD iPSCs and their derived neurons. Thus, FOXO4, plays an important role in regulating proteasome activity in HD iPSCs and their derived neural cells.

As the UPS plays a crucial role in regulation of cell proliferation and differentiation (17,26), elevated proteasome activity in HD iPSCs is likely required for dealing with mutant Htt and for maintaining self-renewal and pluripotency of the cells. Expression of mutant Htt has been shown to alter

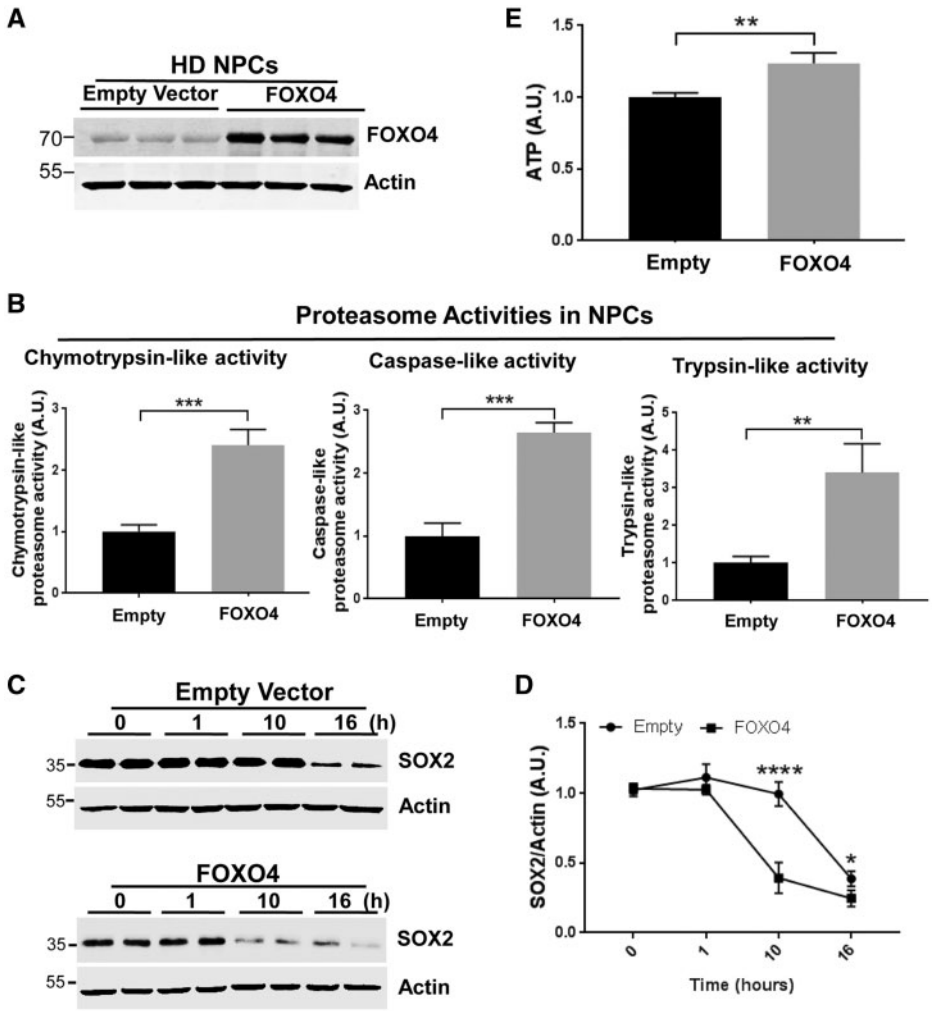

Figure 4. Overexpression of FOXO4 in HD iPSC-derived NPCs increases proteasome activity. (**A**) Western blot analysis of FOXO4 expressions in HD (99Q) NPCs transfected with a FOXO4 plasmid. (**B**) The three types of proteasome activity in FOXO4 overexpression cells. (**C**) CHX chase analysis of SOX2 degradation in HD NPCs transfected either with an empty vector or with a FOXO4 plasmid. The transfected HD cells were treated with 200 μg/ml CHX before cell lysates were collected at the indicated time points for western blot analysis of SOX2 protein levels. Top panel, SOX2 protein degradation in the control-transfected HD NPCs; lower panel, SOX2 protein degradation in FOXO4-transfected HD NPCs at the indicated time points. (**D**) Quantification of the relative levels of SOX2 shown in (**C**). (E) ATP level in FOXO4 overexpression cells. Data are shown as mean ± SD; $n = 3$. *$P < 0.05$, **$P < 0.01$, ****$P < 0.0001$.

mitochondrial structures and functions, leading to impaired energy metabolism and increased production of reactive oxygen species (27). It is conceivable that HD iPSCs contain higher levels of misfolded proteins and thus produce more free radicals than the WT iPSCs. Thus, the HD iPSCs should produce more Ub proteins. In fact, the Ub protein level in HD iPSCs did not differ from that in the WT iPSCs, which might be attributed to the increased proteasome activity in the HD iPSCs. This was further supported by enhanced degradation of a proteasome substrate, SOX2, in HD iPSCs. These results may explain, at least partially, why HD stem cells do not show mutant Htt aggregates and toxicity (28). On the other hand, high proteasome activity found in HD iPSCs may reflect an increased demand for maintaining the gene regulation network to control self-renewal and pluripotency of HD iPSCs, including removal of tissue-specific transcription factors and RNA polymerase II to prevent binding to their target genes and to repress cell differentiation (29).

FOXO transcription factors have been implicated in numerous neurodegenerative disorders, but their exact roles in these diseases remain obscure (30). Our data strongly support a critical role of FOXO4 in modulating proteasome activity observed in HD iPSCs and their derived neural cells. Among the four FOXO members, only FOXO4 protein level is closely associated with proteasome activity alteration. Although both FOXO1 and FOXO4 protein levels showed an increase in HD iPSCs, our knockdown experiments excluded the possibility that FOXO1 contributed to increased proteasome activity. Moreover, overexpression of FOXO4 but not FOXO1 dramatically enhanced proteasome activity and cell survival in neural cells. Previous studies have indicated that PSMD11, a 19 S non-ATPase proteasome subunit, functions as a molecular clamp holding the 20 S proteasome core and the 19 S regulatory particle together (31). In embryonic stem cells, PSMD11 appears to play an important role in upregulating proteasome activity (17). It is possible that increased FOXO4 mediates elevated proteasome activity likely through enhancing 26 S/30 S proteasome assembly via PSMD11 in the HD iPSCs. Indeed, our data support this possibility (unpublished data). However, it remains largely unknown what other genes are regulated by FOXO4, leading to altered UPS functionality.

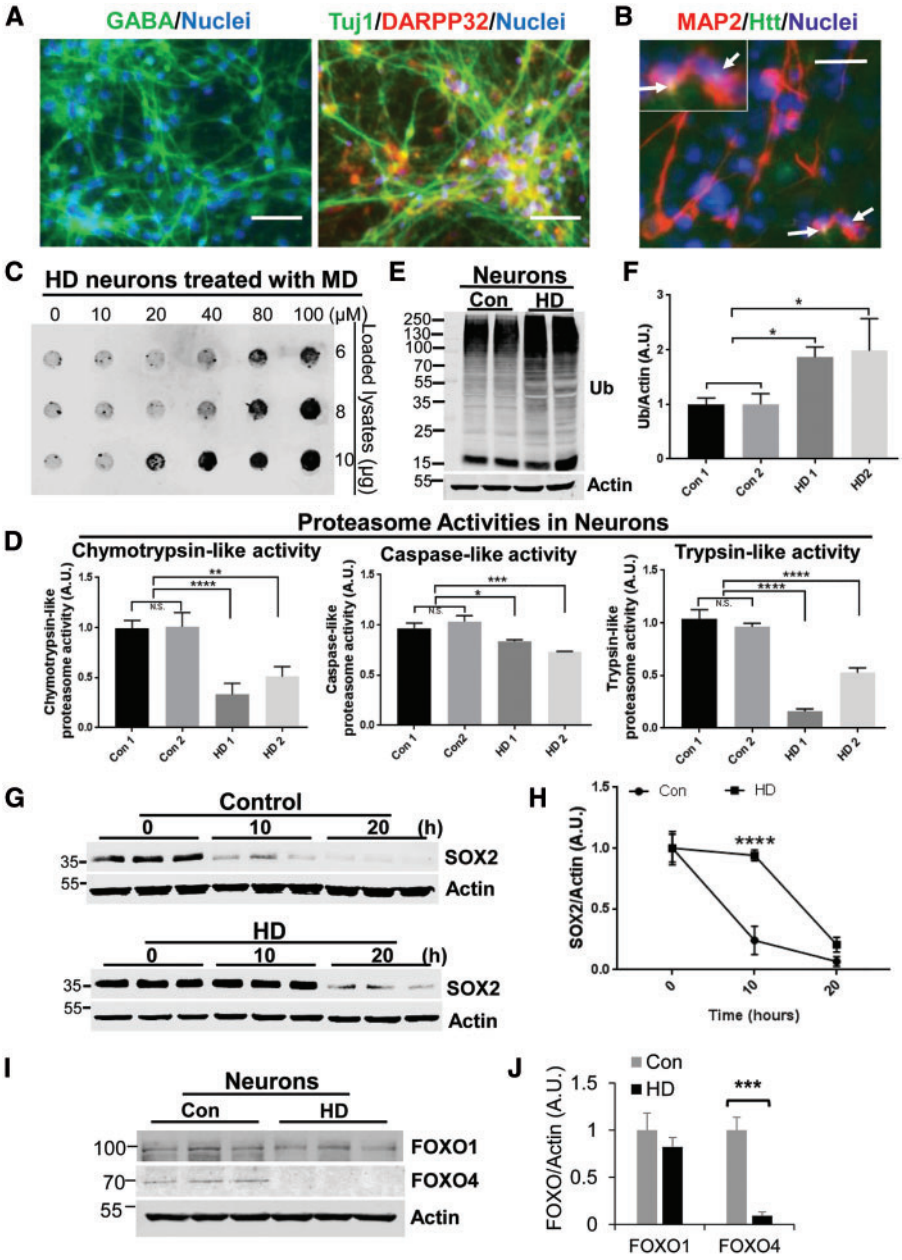

Figure 5. HD iPSC-derived neurons show reduced proteasome activity and decreased FOXO4 expression compared with WT iPSC-derived neurons. (**A**) The differentiated neurons were positive in GABA, Tuj1 and DARPP32 expressions. Hoechst 33342 was used for staining nuclei. Scale bar, 25 μm. (**B**) Immunofluorescence of HD-derived 99Q neuronal cells following oxidative stress treatment (20 μM MD for 6 h) showed Htt aggregates in cells stained with the EM48 mutant Htt antibody. Arrows, aggregates. Scale bar, 25 μm. (**C**) Filter trap assay to analyze protein aggregates in HD neurons (99Q) treated with different concentrations of MD as indicated. (**D**) Three types of proteasome activity in two lines of WT and two lines of HD iPSC-derived neurons. Data are shown as mean ± SD; $n = 3$. $^{*}P < 0.05$, $^{**}P < 0.01$, $^{***}P < 0.001$, $^{****}P < 0.0001$. (**E**) Western blot analysis of Ub expression in neuronal cells. (**F**) Quantitative results measured from experiment (E). Data are shown as mean ± SD; $n = 3$. $^{*}P < 0.05$. (**G**) CHX chase analysis of SOX2 degradation in control and HD neurons at the indicated time points. Control or HD neurons were treated with 100 μg/ml CHX and the cell lysates were collected at the indicated time points for Western blot analysis of SOX2 protein levels. Top panel, SOX2 protein degradation in the control-neurons; lower panel, SOX2 protein degradation in HD neurons at the indicated time points. (**H**) Quantification of the relative levels of SOX2 shown in (G). Data are shown as mean ± SD; $n = 3$. $^{****}P < 0.0001$. (**I**) Western blot analysis of FOXO1 and FOXO4 protein levels in neurons. (**J**) Quantitative results measured from (I). Data are shown as mean ± SD; $n = 3$. $^{***}P < 0.001$.

Our results also indicate that the HD iPSCs generated here are a valuable tool for studying HD. Despite several previous reports of HD iPSCs, mutant Htt aggregates in their derived neurons have not been reported. Following neuronal differentiation, the neurons derived from HD iPSCs exhibited reduced viability following oxidative challenge (unpublished observation), indicating the effect of mutant Htt neurotoxicity (32–34). This result is in agreement with previous observations showing that HD iPSC-derived neurons are more vulnerable to cellular stressors and to the withdrawal of brain derived neurotrophic factor than are normal control cells (35,36). Similar to these previous reports, we did not see microscope-detectable mutant Htt aggregates in HD iPSC-derived neurons in the normal culture condition without any oxidative stress treatment.

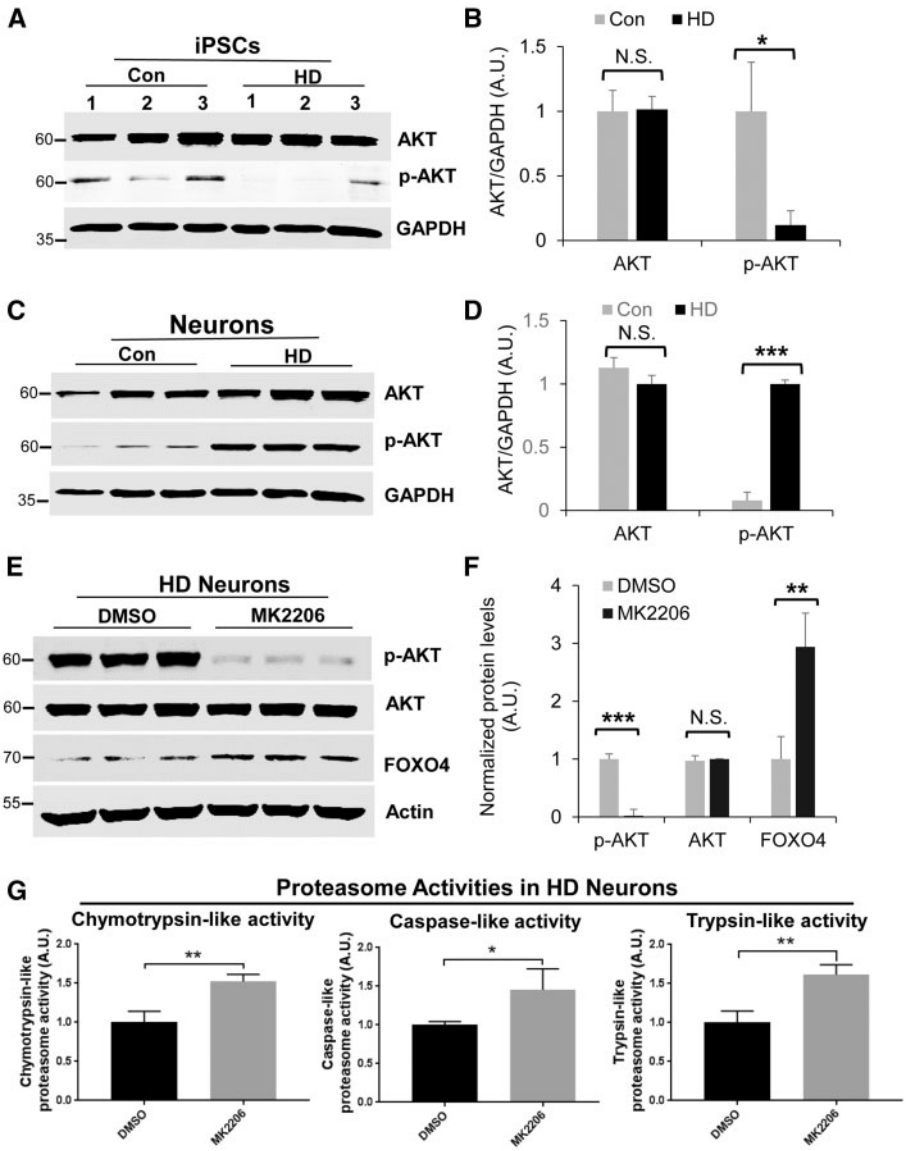

Figure 6. HD iPSCs show reduced levels of AKT activation while HD iPSC-derived neurons exhibit increased levels of AKT activation. (**A**) Western blot analysis of total AKT and p-AKT in WT (Con) and HD iPSCs. (**B**) Quantitative results measured from **(A)**. Data are shown as mean ± SD; $n = 3$. $^{*}P < 0.05$. (**C**) Western blot analysis of total AKT and p-AKT in Con and HD iPSC-derived neurons. (**D**) Quantitative results measured from (C). Data are shown as mean ± SD; $n = 3$. $^{***}P < 0.001$. (**E**) Inhibition of AKT increases FOXO4 level. Western blot analysis of phosphorylated AKT, total AKT and FOXO4 protein levels following treatment of neurons with a selective AKT inhibitor, MK-2206 (5 μM) for 15 h. (**F**) Quantitative results measured from (E). Data are shown as mean ± SD; $n = 3$. $^{**}P < 0.01$, $^{***}P < 0.001$. (**G**) Inhibition of AKT increases proteasome activities. Data are shown as mean ± SD; $n = 3$. $^{*}P < 0.05$, $^{**}P < 0.01$.

Intriguingly, in presence of an oxidative stress inducer, we observed small but evident protein aggregates in the juvenile HD iPSC-derived neurons. The filter trap assay supports the hypothesis that dose-dependent oxidative stress facilitates formation of mutant Htt aggregates.

The serine/threonine kinase, AKT, has been shown to be a major regulator of FOXOs (37). In addition to mediating phosphorylation, AKT activation also promotes degradation of FOXO proteins (24). However, previous studies on AKT activity in HD were inconclusive. In a knock-in mouse model, increased levels of activated AKT were detected in the striatum and cultured HD striatal cells compared with their wild type counterparts, while no changes in phosphorylated FOXO1 levels were detected (38). Another study has shown that both the activated and total AKT levels were reduced in a rat HD model and in post-mortem brain extracts from patients with HD (39). Additionally, unchanged AKT activation has been reported in HD cells (40), but increased FOXO3a levels were detected in HD cells (41). Here our results have shown that activated AKT levels were reduced in HD iPSCs, whereas they were increased in HD neurons. It is likely that the reduced AKT activation level is attributed to increased FOXO4 level in HD iPSCs, which in turn upregulates proteasome activity in HD iPSCs (Fig. 7A). In contrast, the elevated AKT activation found in HD iPSC-derived neurons may be responsible for the downregulation of FOXO4 protein level, leading to reduction of proteasome activity (Fig. 7B). Importantly, inhibition of AKT by MK-2206 increased both FOXO4 level and proteasome activity, which strongly support the role of AKT in regulating FOXO4 protein level. Although

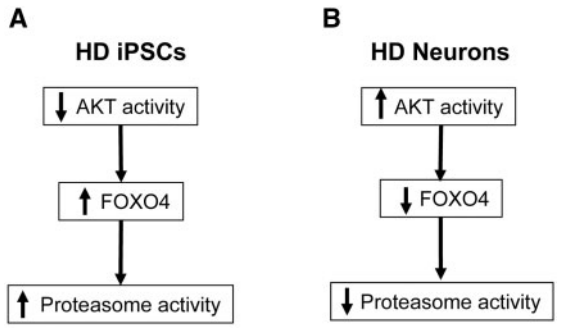

Figure 7. Hypothetical models to explain FOXO4 mediated regulation of proteasome activity in both HD iPSCs and their derived neurons. (**A**) In HD iPSCs, activated AKT levels are reduced, leading to upregulation of FOXO4 and elevated proteasome activity. (**B**) In HD iPSC-derived neurons, activated AKT levels are increased, resulting in downregulation of FOXO4 and decreased proteasome activity.

FOXO4 level was reduced in HD NPCs, AKT activation level did not change in the cells, suggesting that decreased FOXO4 in HD NPCs is independent of AKT signaling pathway.

In summary, we have generated several HD iPSC lines and identified FOXO4 as a modulator of proteasome activity in HD iPSCs and their derived neural cells. Our data also indicate that FOXO4-mediated proteasome activity alterations are likely to be modulated by AKT signaling pathway in HD iPSCs and their derived neurons (Fig. 7A and B). These results not only shed novel light on the role of the proteasome in reprogramming HD somatic cells into iPSCs but also enhance our understanding of HD pathogenesis.

Materials and Methods

Generation of non-integrating iPSCs with control and HD patient fibroblasts

The human fibroblast cells used for reprogramming were obtained from the Coriell Institute for Medical Research (Camden, NJ, USA). Reprogramming of the two control cell lines (16Q and18Q) were conducted using nucleofection (VPD-1001 with program U-20, Amaxa, Walkersville, MD, USA) of the three plasmids, pEP4EO2SEN2K, pEP4EO2SET2K, and pCEP4-LM2L (gifts from Dr. James Thomas, Addgene #20925, #20926, #20927, respectively), into the fibroblast cells with the methods as previously reported (18,19). For generation of another line of control iPSC and several HD iPS cell lines (46Q, 69Q, 70Q, and 99Q), human fibroblast cells were electroporated with the plasmids pCXLE-hOCT3/4-shp53-F, pCXLE-hSK, and pCXLE-hUL (gifts from Dr. Shinya Yamanaka, Addgene #27077, #27078, #27080, respectively) using the Neon Transfection System (Life Technologies, Carlsbad, CA, USA), as previously described (20). Three days after the transfection, the culture medium was changed to TeSR-E7 (STEMCELL Technologies, Vancouver, BC, Canada). The medium was changed daily for up to 30 days before colonies were picked and propagated. The newly derived iPSC colonies were maintained on Matrigel (Corning, Corning, NY, USA) in mTeSR1 (STEMCELL Technologies, Vancouver, Canada) medium at 37 °C, 5% CO_2 and were split every 5–7 days.

Karyotype analysis

iPSCs were treated with colcemid (0.1 μg/ml, Life Technologies) for 2 h before the cells were collected using trypsin detachment. After incubation of the cells with 0.075 M KCl for 20 min, the cells were fixed in 3: 1 methanol: glacial acetic acid, as previously described (42). Standard G-banding and chromosome analysis were carried out either by the Sanford Medical Genetics Laboratory (Sioux Falls, SD, USA) or by the WiCell Research Institute (Madison, WI, USA).

PCR analysis of episomal vectors

We followed the previously described methods to isolate genomic DNA and perform PCR analysis of the episomal vector genes (19). The fibroblasts transfected with the combined vectors but only cultured for 2 days were used as a positive control.

Teratoma formation assay

To examine the *in vivo* differentiation potential of iPSCs, teratomas formation assay was employed. Teratomas are benign tumors characterized by their rapid cell proliferation *in vivo* and by their chaotic mixture of tissues including semi-semblances of organs, teeth, hair, muscle, cartilage, and even bone. Briefly, the iPSCs were grown on Matrigel in mTeSR1 medium and were collected in 1: 1 of Matrigel (Corning): DMEM/F12 (Life Technologies). The iPSCs were then injected into the testis capsule of 6-week-old immunocompromised SCID-beige mice (Harlan, Indianapolis, IN, USA) using the previously described methods (43). After 10 to 12 weeks of injection, teratomas were collected and fixed in 10% formalin (Fisher, Pittsburgh, PA, USA). Samples were embedded in paraffin and processed with hematoxylin and eosin staining. Images were taken with an Amscope microscope equipped with the ToupView software (Irvine, California, USA).

Determination of CAG repeat numbers in fibroblasts and iPSCs

Genomic DNAs were extracted from human fibroblasts or iPSCs using a genomic DNA purification kit (Genelink, Hawthorne, NY, USA) according to the manufacturer's instructions. The genomic DNAs were then submitted to the Emory Genetics Laboratory (Decatur, Georgia, USA) to determine CAG repeat lengths.

Neural induction and neuronal differentiation

For neuronal induction, iPSCs were first differentiated into neural progenitor cells (NPCs) using an embryoid body-based protocol. Briefly, iPSCs were detached using Accutase at 37 °C and plated into the AggreWell™ 800 (STEMCELL Technologies) in AggreWell medium (STEMCELL Technologies) to form embryoid bodies. After 5 days, embryoid bodies were re-plated and cultured in a neural induction medium. NPCs were then obtained following rosette selection using STEMdiff ™ neural rosette selection medium (STEMCELL Technologies) and cultured in neural induction medium supplemented with purmorphamine (StemGent) and B27 (Invitrogen).

To differentiate NPCs into neurons, we used a previously described method (44). Briefly, the NPCs were cultured in a neuronal differentiation medium composed of neural basal medium (Life Technologies) supplemented with non-essential amino acids (Life Technologies), N2 supplemental medium (Life Technologies), 1 μM Cyclic adenosine monophosphate (cAMP, Santa Cruz Biotechnology), 10 ng/ml BDNF (Peprotech, Rocky Hill, NJ, USA), 10 ng/ml GDNF (Peprotech), and 10 ng/ml IGF1

(Peprotech). The neuronal differentiation media were changed every 3–4 days. The cells were differentiated for at least 60 days before being used for experiments. For drug treatment, cells were incubated with different concentrations of a free radical inducer, menadione (Sigma, St Louis, MO, USA) (23) for 6 h and then collected either for immunostaining or for the filter trap assay.

Lentiviral FOXO-siRNA preparation and knockdown experiments

We followed the previously described method to package and produce lentiviral particles (45). Briefly, 293 T cells were plated in 10 cm dishes and cultured in DMEM supplement with 10% FBS at 37 °C in 5% CO_2. The next day, when cells reached 70% confluence, cells were transfected with 3 μg pCMV-VSV-G, 7.5 μg pCMV-dR8.2-dvpr, and 8 μg four-mixed plenti-FOXO1 or -FOXO4-siRNA plasmids (2 μg for each plenti-siRNA plasmid) by using Lipofectamine 2000 transfection reagent (Invitrogen). The medium was replaced with fresh complete medium 24 h after the transfection. The medium containing FOXO1- and FOXO4 siRNAs pseudolentiviruses were collected 48 and 72 h following the transfection and then ultracentrifuged in a SW27 rotor (Beckman Coulter) at 23, 000 × g for 5 h. Lentiviral pellets were resuspended with 100–200 μl DMEM. The lentiviruses were then aliquoted and stored at −70 °C. To infect iPSCs with lentiviral FOXO1 or FOXO4 siRNAs, 99Q HD iPSCs were incubated with the viral particles for 72 h in presence of 8 μg/ml polybrene before the cells were collected for Western blot analysis of FOXO1 or FOXO4 protein expressions and proteasome activity.

Cell transfection

NPCs were cultured in 12-well plates in the NPC Complete Medium (STEMCELL Technologies). The cells were transfected with Flag-tagged FOXO1 or FOXO4 using Lipofectamine 3000 transfection kit (Invitrogen) by following the manufacturer's instruction. After 48 h following the transfection, the FOXO1 and FOXO4 transfected cells were collected for western blot analysis, proteasome activity assay, and cell viability assay.

ATP assay

ATP assay was performed to evaluate cell viability using an ATP Bioluminescence assay kit CLS II (Sigma) according to the manufacturer provided protocol.

Proteasome activity assay

Cells were lysed in proteasome activity assay buffer (50 mM Tris-HCl, pH 7.5, 250 mM sucrose, 5 mM $MgCl_2$, 0.5 mM EDTA, 2 mM ATP and 1 mM dithiothreitol) by passing them ten times through a 27-gauge needle attached to a 1 ml syringe. The BCA protein assay kit (Fisher Scientific, Hampton, NH) was used to determine the protein concentration. Approximately, 20 μg of total proteins from cell lysates was used for detection. The fluorogenic substrate Suc-Leu-Leu-Val-Tyr-AMC (40 μM) was used to measure the chymotrypsin-like activity of the proteasome. Z-Leu-Leu-Glu-AMC (40 μM) was used to measure the caspase-like activity of proteasome and the Boc-Leu-Arg-Arg-AMC (40 μM) was used to measure the trypsin-like activity of proteasome. Fluorescence intensity was measured at 380 nm excitation and 460 nm emission by using a plate reader (PerkinElmer, Waltham, MA, USA).

Immunocytochemical staining and fluorescence microscopy

Immunocytochemistry was performed according to previously described methods (46). The following primary antibodies and dilutions were used: anti-Nanog 1: 100 (PeproTech), anti-OCT4A 1: 400 (Cell Signaling, Danvers, MA, USA), anti-SOX2 1: 1000 (Millipore, Billerica, MA), anti-TRA-1-60 1: 500 (Millipore), anti-SSEA4 1: 500 (Cell Signaling), anti-Tuj1 1: 200 (Cell Signaling), anti-DARPP-32 1: 50 (Santa Cruz Biotechnology, Santa Cruz, CA), anti-GABA 1: 1000 (Millipore), anti-EM48 1: 100 (Millipore), anti-MAP2 1: 100 (Cell Signaling), anti-Nestin 1: 200 (Millipore), and anti-Doublecortin 1: 50 (Santa Cruz Biotechnology). The secondary antibodies were prepared as previously described (47,48). The DNA-binding dye Hoechst 33342 was used to label nuclei. Images were captured with a fluorescence microscope equipped with the AxioVision 4.8 software (Carl Zeiss, Jena, Germany).

Western blotting

We employed previously described methods to prepare cell lysates and perform the sodium dodecyl sulfate (SDS) polyacrylamide gel electrophoresis (PAGE) to separate proteins (48,49). After proteins were transferred onto a nitrocellulose or polyvinylidene difluoride (PVDF) membrane, they were immunoprobed either with an anti-ubiquitin antibody (1: 1000, Cell Signaling), anti-FOXO1 antibody (1: 1000, Cell Signaling), anti-FOXO3a antibody (1: 1000, Cell Signaling), anti-FOXO4 antibody (1: 1000, Cell Signaling), anti-FOXO6 antibody (1: 1000, OriGene), anti-hSOX2 (1: 1000, R&D Systems), anti-p-AKT (1: 1000, Cell Signaling), anti-AKT (1: 1000, Cell Signaling), anti-GAPDH (1: 1000, Cell Signaling), or with an anti-actin antibody (1: 500, Santa Cruz Biotechnology) at 4 °C overnight. After washing for three times with the Tris-buffered saline containing 0.1% Tween-20, the anti-rabbit, anti-mouse, or anti-goat IRDye 800CW or IRDye 680RD secondary antibodies (LI-COR, Lincoln, NE, USA) was utilized. The bands on membranes were imaged by using image studio software (LI-COR). Protein band intensities were quantified using the UN-SCAN-IT gel software (Silk Scientific, Orem, UT, USA).

Cycloheximide (CHX) chase assay

WT and HD iPSCs, NPCs and neuronal cells were cultured in 12-well plates. The cells were treated with 50 (in iPSCs), 100 (in neurons), or 200 μg/ml CHX (in NPCs), and total protein lysates were collected at different time points and subjected to immunoblotting for SOX2 protein (1: 1, 000, R&D Systems) and actin (1: 500, Santa Cruz Biotechnology).

Filter trap assay of protein aggregates

Filter trap assay of protein aggregates was based on a previously described method (47). Briefly, neurons were collected in a cell lysis buffer (10 mM Tris pH 8.0, 150 mM NaCl, and 2% SDS). Then 200 μl samples were boiled for 3 min and loaded onto a cellulose acetate membrane that was placed on the Dot-Blot apparatus (Bio-Rad) connected with a vacuum pump. After filtration of the lysates, the membrane was washed twice before being probed using the EM48 antibody by Western blot.

MK-2206 treatment

HD neurons were treated with 5 μM MK-2206 (Selleck Chemicals, TX, USA) for 15 h before cell lysates were collected for western blot analysis or proteasome activity assay.

Statistical analysis

Statistical analysis was conducted using the PRISM 7.0 (GraphPad Software, La Jolla, CA, USA). Student's t-test (two-tailed) was used for comparison between two groups. For those data comprised of more than two groups, data were analyzed with the one-factor analysis of variance (ANOVA) followed by a Tukey post hoc test or two-way ANOVA using the statistical analysis software PRISM 7.0. Data were presented as means ± standard deviation and $p < 0.05$ was considered to be statistically significant.

Acknowledgements

We would like to thank Dr. James A. Thomson at the University of Wisconsin-Madison and Dr. Junying Yu at the Cellular Dynamics International, Inc., Madison, WI for support and technical assistance, and Suchun Zhang at the University of Wisconsin for kind suggestions on neuronal differentiation. We would also like to thank Drs. Khosrow Rezvani and Pasquale Manzerra at the University of South Dakota for providing reagents or equipment.

Conflict of Interest statement. None declared.

Funding

University of South Dakota and National Institute of Health (R15NS071459).

References

1. Bates, G.P. (2005) History of genetic disease: the molecular genetics of Huntington disease - a history. *Nat. Rev. Genet.*, **6**, 766–773.
2. MacDonald, M.E. and Gusella, J.F. (1996) Huntington's disease: translating a CAG repeat into a pathogenic mechanism. *Curr. Opin. Neurobiol.*, **6**, 638–643.
3. Walker, F.O. (2007) Huntington's disease. *Lancet*, **369**, 218–228.
4. Li, X.J. (1999) The early cellular pathology of Huntington's disease. *Mol. Neurobiol.*, **20**, 111–124.
5. Vonsattel, J.P. and DiFiglia, M. (1998) Huntington disease. *J. Neuropathol. Exp. Neurol.*, **57**, 369–384.
6. Demartino, G.N. and Gillette, T.G. (2007) Proteasomes: machines for all reasons. *Cell*, **129**, 659–662.
7. Li, X., Thompson, D., Kumar, B. and DeMartino, G.N. (2014) Molecular and cellular roles of PI31 (PSMF1) protein in regulation of proteasome function. *J. Biol. Chem.*, **289**, 17392–17405.
8. Kim, Y.C., Li, X., Thompson, D. and DeMartino, G.N. (2013) ATP binding by proteasomal ATPases regulates cellular assembly and substrate-induced functions of the 26 S proteasome. *J. Biol. Chem.*, **288**, 3334–3345.
9. Seo, H., Sonntag, K.C. and Isacson, O. (2004) Generalized brain and skin proteasome inhibition in Huntington's disease. *Ann. Neurol.*, **56**, 319–328.
10. Wang, J., Wang, C.E., Orr, A., Tydlacka, S., Li, S.H. and Li, X.J. (2008) Impaired ubiquitin-proteasome system activity in the synapses of Huntington's disease mice. *J. Cell Biol.*, **180**, 1177–1189.
11. Bennett, E.J., Shaler, T.A., Woodman, B., Ryu, K.Y., Zaitseva, T.S., Becker, C.H., Bates, G.P., Schulman, H. and Kopito, R.R. (2007) Global changes to the ubiquitin system in Huntington's disease. *Nature*, **448**, 704–708.
12. Diaz-Hernandez, M., Hernandez, F., Martin-Aparicio, E., Gomez-Ramos, P., Moran, M.A., Castano, J.G., Ferrer, I., Avila, J. and Lucas, J.J. (2003) Neuronal induction of the immunoproteasome in Huntington's disease. *J. Neurosci.*, **23**, 11653–11661.
13. Bett, J.S., Goellner, G.M., Woodman, B., Pratt, G., Rechsteiner, M. and Bates, G.P. (2006) Proteasome impairment does not contribute to pathogenesis in R6/2 Huntington's disease mice: exclusion of proteasome activator REGgamma as a therapeutic target. *Hum. Mol. Genet.*, **15**, 33–44.
14. Seo, H., Kim, W. and Isacson, O. (2008) Compensatory changes in the ubiquitin-proteasome system, brain-derived neurotrophic factor and mitochondrial complex II/III in YAC72 and R6/2 transgenic mice partially model Huntington's disease patients. *Hum. Mol. Genet.*, **17**, 3144–3153.
15. Webb, A.E. and Brunet, A. (2014) FOXO transcription factors: key regulators of cellular quality control. *Trends Biochem. Sci.*, **39**, 159–169.
16. van der Horst, A. and Burgering, B.M. (2007) Stressing the role of FoxO proteins in lifespan and disease. *Nat. Rev. Mol. Cell Biol.*, **8**, 440–450.
17. Vilchez, D., Boyer, L., Morantte, I., Lutz, M., Merkwirth, C., Joyce, D., Spencer, B., Page, L., Masliah, E., Berggren, W.T. *et al.* (2012) Increased proteasome activity in human embryonic stem cells is regulated by PSMD11. *Nature*, **489**, 304–308.
18. Yu, J., Hu, K., Smuga-Otto, K., Tian, S., Stewart, R., Slukvin, I.I. and Thomson, J.A. (2009) Human induced pluripotent stem cells free of vector and transgene sequences. *Science*, **324**, 797–801.
19. Yu, J., Chau, K.F., Vodyanik, M.A., Jiang, J. and Jiang, Y. (2011) Efficient feeder-free episomal reprogramming with small molecules. *PLoS One*, **6**, e17557.
20. Okita, K., Matsumura, Y., Sato, Y., Okada, A., Morizane, A., Okamoto, S., Hong, H., Nakagawa, M., Tanabe, K., Tezuka, K. *et al.* (2011) A more efficient method to generate integration-free human iPS cells. *Nat. Methods*, **8**, 409–412.
21. Wang, J., Zhang, Y., Hou, J., Qian, X., Zhang, H., Zhang, Z., Li, M., Wang, R., Liao, K., Wang, Y. *et al.* (2016) Ube2s regulates Sox2 stability and mouse ES cell maintenance. *Cell Death Differ.*, **23**, 393–404.
22. Ouimet, C.C., Miller, P.E., Hemmings, H.C., Jr., Walaas, S.I. and Greengard, P. (1984) DARPP-32, a dopamine- and adenosine 3': 5'-monophosphate-regulated phosphoprotein enriched in dopamine-innervated brain regions. III. Immunocytochemical localization. *J. Neurosci.*, **4**, 111–124.
23. Liu, Y., Lu, L., Hettinger, C.L., Dong, G., Zhang, D., Rezvani, K., Wang, X. and Wang, H. (2014) Ubiquilin-1 protects cells from oxidative stress and ischemic stroke caused tissue injury in mice. *J. Neurosci.*, **34**, 2813–2821.
24. Huang, H. and Tindall, D.J. (2011) Regulation of FOXO protein stability via ubiquitination and proteasome degradation. *Biochim. Biophys. Acta*, **1813**, 1961–1964.
25. Hirai, H., Sootome, H., Nakatsuru, Y., Miyama, K., Taguchi, S., Tsujioka, K., Ueno, Y., Hatch, H., Majumder, P.K., Pan, B.S. *et al.* (2010) MK-2206, an allosteric Akt inhibitor, enhances

antitumor efficacy by standard chemotherapeutic agents or molecular targeted drugs in vitro and in vivo. *Mol. Cancer Ther.*, **9**, 1956–1967.
26. Hernebring, M., Fredriksson, A., Liljevald, M., Cvijovic, M., Norrman, K., Wiseman, J., Semb, H. and Nystrom, T. (2013) Removal of damaged proteins during ES cell fate specification requires the proteasome activator PA28. *Sci. Rep.*, **3**, 1381.
27. Kunkanjanawan, T., Carter, R., Ahn, K.S., Yang, J., Parnpai, R. and Chan, A.W. (2017) Induced pluripotent HD monkey stem cells derived neural cells for drug discovery. *SLAS Discov.*, **22**, 696–705.
28. Nasir, J., Floresco, S.B., O'Kusky, J.R., Diewert, V.M., Richman, J.M., Zeisler, J., Borowski, A., Marth, J.D., Phillips, A.G. and Hayden, M.R. (1995) Targeted disruption of the Huntington's disease gene results in embryonic lethality and behavioral and morphological changes in heterozygotes. *Cell*, **81**, 811–823.
29. Szutorisz, H., Georgiou, A., Tora, L. and Dillon, N. (2006) The proteasome restricts permissive transcription at tissue-specific gene loci in embryonic stem cells. *Cell*, **127**, 1375–1388.
30. Neri, C. (2012) Role and therapeutic potential of the pro-longevity factor FOXO and its regulators in neurodegenerative disease. *Front. Pharmacol.*, **3**, 15.
31. Pathare, G.R., Nagy, I., Bohn, S., Unverdorben, P., Hubert, A., Korner, R., Nickell, S., Lasker, K., Sali, A., Tamura, T. *et al.* (2012) The proteasomal subunit Rpn6 is a molecular clamp holding the core and regulatory subcomplexes together. *Proc. Natl. Acad. Sci. U. S. A*, **109**, 149–154.
32. Carter, R.L., Chen, Y., Kunkanjanawan, T., Xu, Y., Moran, S.P., Putkhao, K., Yang, J., Huang, A.H., Parnpai, R. and Chan, A.W. (2014) Reversal of cellular phenotypes in neural cells derived from Huntington's disease monkey-induced pluripotent stem cells. *Stem Cell Reports*, **3**, 585–593.
33. Chan, A.W., Cheng, P.H., Neumann, A. and Yang, J.J. (2010) Reprogramming Huntington monkey skin cells into pluripotent stem cells. *Cell Reprogram*, **12**, 509–517.
34. Bradford, J., Shin, J.Y., Roberts, M., Wang, C.E., Li, X.J. and Li, S. (2009) Expression of mutant huntingtin in mouse brain astrocytes causes age-dependent neurological symptoms. *Proc. Natl. Acad. Sci. U. S. A*, **106**, 22480–22485.
35. Consortium, H.D.i. (2012) Induced pluripotent stem cells from patients with Huntington's disease show CAG-repeat-expansion-associated phenotypes. *Cell Stem Cell*, **11**, 264–278.
36. Mattis, V.B., Tom, C., Akimov, S., Saeedian, J., Ostergaard, M.E., Southwell, A.L., Doty, C.N., Ornelas, L., Sahabian, A., Lenaeus, L. *et al.* (2015) HD iPSC-derived neural progenitors accumulate in culture and are susceptible to BDNF withdrawal due to glutamate toxicity. *Hum. Mol. Genet.*, **24**, 3257–3271.
37. Brunet, A., Bonni, A., Zigmond, M.J., Lin, M.Z., Juo, P., Hu, L.S., Anderson, M.J., Arden, K.C., Blenis, J. and Greenberg, M.E. (1999) Akt promotes cell survival by phosphorylating and inhibiting a Forkhead transcription factor. *Cell*, **96**, 857–868.
38. Gines, S., Ivanova, E., Seong, I.S., Saura, C.A. and MacDonald, M.E. (2003) Enhanced Akt signaling is an early pro-survival response that reflects N-methyl-D-aspartate receptor activation in Huntington's disease knock-in striatal cells. *J. Biol. Chem.*, **278**, 50514–50522.
39. Colin, E., Regulier, E., Perrin, V., Durr, A., Brice, A., Aebischer, P., Deglon, N., Humbert, S. and Saudou, F. (2005) Akt is altered in an animal model of Huntington's disease and in patients. *Eur. J. Neurosci.*, **21**, 1478–1488.
40. Gines, S., Paoletti, P. and Alberch, J. (2010) Impaired TrkB-mediated ERK1/2 activation in huntington disease knock-in striatal cells involves reduced p52/p46 Shc expression. *J. Biol. Chem.*, **285**, 21537–21548.
41. Kannike, K., Sepp, M., Zuccato, C., Cattaneo, E. and Timmusk, T. (2014) Forkhead transcription factor FOXO3a levels are increased in Huntington disease because of overactivated positive autofeedback loop. *J. Biol. Chem.*, **289**, 32845–32857.
42. Howe, B., Umrigar, A. and Tsien, F. (2014) Chromosome preparation from cultured cells. *J. Vis.Exp.*, **83**, e50203.
43. Peterson, S.E., Tran, H.T., Garitaonandia, I., Han, S., Nickey, K.S., Leonardo, T., Laurent, L.C. and Loring, J.F. (2011) Teratoma generation in the testis capsule. *J. Vis. Exp.*, **57**, e3177.
44. Liu, Y., Liu, H., Sauvey, C., Yao, L., Zarnowska, E.D. and Zhang, S.C. (2013) Directed differentiation of forebrain GABA interneurons from human pluripotent stem cells. *Nat. Protoc.*, **8**, 1670–1679.
45. Liu, Y., Qiao, F. and Wang, H. (2016) Enhanced proteostasis in post-ischemic stroke mouse brains by ubiquilin-1 promotes functional recovery. *Cell Mol Neurobiol.*, DOI: 10.1007/s10571-016-0451-3.
46. Liu, Y., Xue, Y., Ridley, S., Zhang, D., Rezvani, K., Fu, X.-D., Wang, H. and Smith, W. (2014) Direct reprogramming of Huntington's disease patient fibroblasts into neuron-like cells leads to abnormal neurite outgrowth, increased cell death, and aggregate formation. *PLoS One*, **9**, e109621.
47. Dong, G., Ferguson, J.M., Duling, A.J., Nicholas, R.G., Zhang, D., Rezvani, K., Fang, S., Monteiro, M.J., Li, S., Li, X.-J. and Wang, H. (2011) Modeling pathogenesis of Huntington's disease with inducible neuroprogenitor cells. *Cell. Mol. Neurobiol.*, **31**, 737–747.
48. Dong, G., Gross, K., Qiao, F., Ferguson, J., Callegari, E.A., Rezvani, K., Zhang, D., Gloeckner, C.J., Ueffing, M. and Wang, H. (2012) Calretinin interacts with huntingtin and reduces mutant huntingtin-caused cytotoxicity. *J. Neurochem.*, **123**, 437–446.
49. Dong, G., Callegari, E.A., Gloeckner, C.J., Ueffing, M. and Wang, H. (2012) Prothymosin-alpha interacts with mutant huntingtin and suppresses its cytotoxicity in cell culture. *J. Biol. Chem.*, **287**, 1279–1289.